ResearchGate

See discussions, stats, and author profiles for this publication at: https://www.researchgate.net/publication/222463951

Synthesis and characterization of novel palladium(II) complexes of bis(thiosemicarbazone). Structure, cytotoxic activity and DNA binding of Pd(II)–benzyl bis(thiosemicarbazonate)

ARTICLE *in* JOURNAL OF INORGANIC BIOCHEMISTRY · AUGUST 1999

Impact Factor: 3.44 · DOI: 10.1016/S0162-0134(99)00105-1

CITATIONS
84

READS
29

6 AUTHORS, INCLUDING:

Matesanz ANA
Universidad Autónoma de Madrid
32 PUBLICATIONS **522** CITATIONS
SEE PROFILE

Paloma Navarro
Spanish National Research Council
16 PUBLICATIONS **362** CITATIONS
SEE PROFILE

Available from: Matesanz ANA
Retrieved on: 13 January 2016

ELSEVIER

www.elsevier.nl/locate/jinorgbio

Journal of Inorganic Biochemistry 76 (1999) 29–37

JOURNAL OF Inorganic Biochemistry

Synthesis and characterization of novel palladium(II) complexes of bis(thiosemicarbazone). Structure, cytotoxic activity and DNA binding of Pd(II)-benzyl bis(thiosemicarbazonate)

Ana I. Matesanz [a,1], José M. Pérez [a,1], Paloma Navarro [a], José M. Moreno [b], Enrique Colacio [b], Pilar Souza [a,*]

[a] *Departamento de Química Inorgánica, Facultad de Ciencias, Universidad Autónoma de Madrid, Cantoblanco, 28049 Madrid, Spain*
[b] *Departamento de Química Inorgánica, Facultad de Ciencias, Universidad de Granada, 18071 Granada, Spain*

Received 9 December 1998; received in revised form 17 June 1999; accepted 22 June 1999

Abstract

The preparation of palladium(II) complexes of 3,5-diacyl-1,2,4-triazole bis(thiosemicarbazone) (H_2L^2), 2,6-diacylpyridine bis(thiosemicarbazone) (H_2L^3) and benzyl bis(thiosemicarbazone) (H_2L^4) is described. The new complexes [$PdCl_2(H_2L^2)$] (**1**), [$PdCl_2(H_2L^3)$] (**2**) and [PdL^4]·DMF (**3**) have been characterized by elemental analyses and spectroscopic studies (IR, ^{1}H NMR and UV–Vis). The crystal and molecular structure of PdL^4·DMF (L = bideprotonated form of benzyl bis(thiosemicarbazone)) has been determined by single-crystal X-ray diffraction: green triclinic crystal, $a = 10.258(5)$, $b = 10.595(5)$, $c = 11.189(5)$ Å, $\alpha = 97.820(5)$, $\beta = 108.140(5)$, $\gamma = 105.283(5)°$, space group $P1$, $Z = 1$. The palladium atom is tetracoordinated by four donor atoms (SNNS) from L^4 to form a planar tricyclic ligating system. The testing of the cytotoxic activity of compound **3** against several human, monkey and murine cell lines sensitive (HeLa, Vero and Pam 212) and resistant to *cis*-DDP (Pam-*ras*) suggests that compound **3** might be endowed with important antitumor properties since it shows IC_{50} values in a μM range similar to those of *cis*-DDP [*cis*-diamminedichloroplatinum(II)]. Moreover, compound **3** displays notable cytotoxic activity in Pam-*ras* cells resistant to *cis*-DDP (IC_{50} values of 78 μM versus 156 μM, respectively). On the other hand, the analysis of the interaction of this novel Pd-thiosemicarbazone compound with DNA secondary structure by means of circular dichroism spectroscopy indicates that it induces on the double helix conformational changes different from those induced by *cis*-DDP.
© 1999 Elsevier Science Inc. All rights reserved.

Keywords: Palladium(II) complexes; Bis(thiosemicarbazone); Cytotoxic activity; DNA binding

1. Introduction

Hitherto, the great majority of antitumor metal complexes synthesized and characterized have been structural analogs of cisplatin (*cis*-DDP) [1]. However, there has been a levelling off or perhaps even a decrease in the number of new compounds of this type, possibly because it is beginning to transpire that substantial advances are unlikely to be made with these compounds [2]. At the same time there has been an emergence of new structural types of metallic complexes often with promising activity and able to circumvent cisplatin resistance [3]. Thus, thiosemicarbazide derivatives have raised considerable interest due to their pharmacological properties. In some cases the highest activity is associated with a metal complex [4–9]. For instance, 3-ethoxy-2-oxobutyraldehyde bis(thiosemicarbazonato) copper(II) (abbreviated Cu(KTS)) has proved to be an efficient antitumor agent [10,11].

The relationship between structural and biological properties of metal thiosemicarbazone complexes of different stoichiometries has been reviewed [12]. Several palladium(II) and platinum(II) thiosemicarbazone complexes having potential antitumor activity [13,14] have been recently reported, but surprisingly, only a few complexes with bis(thiosemicarbazone) have been studied [15]. As part of our systematic investigation on the coordination chemistry of thiosemicarbazone derivatives [16–18] we have decided to study bis(thiosemicarbazone) palladium(II) compounds which might have more beneficial biological properties than the thiosemicarbazone ones.

The present paper is devoted to the synthesis and characterization of new palladium(II) complexes with 3,5-diacyl-

* Corresponding author. Fax: +34-91-397-8433; e-mail: souza@jet.es
[1] Both authors contributed equally to this work.

0162-0134/99/$ - see front matter © 1999 Elsevier Science Inc. All rights reserved.
PII S0162-0134(99)00105-1

1,2,4-triazole bis(thiosemicarbazone) (H_2L^2), 2,6-diacetylpyridine bis(thiosemicarbazone) (H_2L^3) and benzyl bis(thiosemicarbazone) (H_2L^4), namely [$Pd(H_2L^2)Cl_2$] (**1**), [$Pd(H_2L^3)Cl_2$] (**2**) and [PdL^4] (**3**). The coordination modes of the H_2L^2, H_2L^3 and H_2L^4 are compared and the crystal structure of [PdL^4] is reported. The isolation and characterization of the latter is important since it reveals geometric similarities with the well-known [Cu(KTS)] complex, and because, to our knowledge, this is the first time that a single crystal structure of a bis(thiosemicarbazone) palladium(II) complex has been reported. We have also tested the cytotoxic activity of this compound. The data indicate that it may be considered a potential antitumor agent in view of the fact that it circumvents cisplatin resistance. Circular dichroism (CD) data show that this novel Pd-bis(thiosemicarbazone) compound induces on the DNA double helix specific conformational changes.

2. Experimental

2.1. Measurements

Infrared spectra (KBr discs) were recorded on a Bomen–Michelson spectrophotometer (4000–400 cm^{-1}) and on a Perkin-Elmer 1650 FT-IR spectrophotometer (400–200 cm^{-1}). Electronic spectra (DMF solution) were recorded on an Ati-Unicam UV2 spectrophotometer. Elemental analyses (C, H, N and S), mass spectra and ^1H NMR were recorded by the Servicio Interdepartamental de Investigación (SIDI) of the Universidad Autónoma de Madrid. CD spectra of CT DNA and CT DNA:drug complexes formed at $r_b = 0.1$ (molar ratio of Pt or Pd bound per nucleotide) were performed in a 1 cm rectangular quartz cell in a JASCO J-600 spectropolarimeter attached to a temperature programmer using a computer for spectral subtraction and noise reduction. The CD analysis was done at 37°C. Each sample was scanned twice in a range of wavelengths between 220 and 320 nm. The generated CD spectra represent the mean of three independent scans. The data are expressed as the mean residual molecular elipticity [θ] in deg cm^2 $dmol^{-1} \times 10^3$.

2.2. Materials

Thiosemicarbazide, 2,6-diacylpyridine, benzyl, hydrazine hydrate, L-lactic acid, lithium chloride, and palladium(II) chloride were commercially available from Aldrich, while lanthanum(III) chloride heptahydrate was from Fluka. All chemicals were used without further purification.

2.2.1. Biological reagents and drugs

100 mm culture and microwell plates were obtained from Nunclon (Roskilde, Denmark); 3-[4,5-dimethylthiazol-2-yl]-2,5-diphenyltetrazolium bromide (MTT) was purchased from Sigma; foetal calf serum (FCS) was supplied by GIBCO-BRL; *cis*-diamminedichloroplatinum(II) (*cis*-DDP) and etoposide ([9-[4,6-*O*-ethylidene-β-D-glucopyranosyl]-oxy]-5,8,8*a*,9-tetrahydro-5-(4-hydroxy-3,5-dimethoxyphenyl)furo[3′,4′:6,7]naphthol[2,3-*d*]-1,3-dioxol-6(5a*H*)-one; 4′-dimethyllepipodophyllotoxin-9-[4,6-*O*-ethylidene-β-D-glucopyranoside]) were purchased from Sigma. Adriamycin (doxorubicin) ((8-*cis*)-10-[3-amino-2,3,6-trideoxy-α-L-lyxo-hexopyranosyloxy]-7,8,9,10-tetrahydro-6,8,11-trihydroxy-8-(hydroxyacetyl)-1-methoxy-5,12-naphtacenedione) was purchased from Tedec-Meiji Farma, as doxorubicin chlorhydrate. *cis*-DDP, adriamycin, etoposide and compound **3** were dissolved in 10 mM $NaClO_4$. Stock solutions of the compounds at a concentration of 1 mg/ml were freshly prepared before use.

2.2.2. Cell lines and culture conditions

HeLa (cervix epithelial human carcinoma line) and Vero (transformed monkey kidney fibroblasts) cells were cultured in DMEM medium supplemented with 10% FCS and 10% new born calf serum, respectively, together with 2 mM glutamine, 100 units/ml penicillin, and 100 mg/ml streptomycin at 37°C in an atmosphere of 95% air and 5% CO_2. Pam 212 (normal murine keratinocytes) and Pam-*ras* [14,19] (murine keratinocites transformed with the H-*ras* oncogene and resistant to *cis*-DDP) were cultured in DMEM medium supplemented with 10% FCS and 2 mM glutamine, 100 units/ml penicillin, and 100 mg/ml streptomycin at 37°C in an atmosphere of 95% air and 5% CO_2. The cultures of tumor cells (HeLa, Vero and Pam-*ras*) were passaged three times per week showing a doubling time between 16 and 24 h, depending on the cell line. Normal murine keratinocytes (Pam 212 cells) were passaged twice weekly showing a doubling time of about 48 h.

2.3. Preparations of the ligands

3,5-Diacyl-1,2,4-triazole bis(thiosemicarbazone) (H_2L^2) and 2,6-diacylpyridine bis(thiosemicarbazone) (H_2L^3) were prepared by reacting equimolar amounts of an ethanolic solution of 3,5-diacyl-1,2,4-triazole [20] for H_2L^2 and 2,6-diacylpyridine for H_2L^3, $LaCl_3 \cdot 7H_2O$, used as template, and thiosemicarbazide. The reaction mixture was heated under reflux for 6 h on a water bath at 60°C. The solid formed was filtered and washed with cold EtOH and Et_2O and dried in vacuo. H_2L^2: *Anal.* Found: C, 28.70; H, 5.10; N, 37.50. $C_8H_{17}N_9O_2S_2$ requires: C, 28.70; H, 5.05; N, 37.60%; mass spectrum: $m/z = 299$, yield = 82%. H_2L^3: *Anal.* Found: C, 40.80; H, 5.00; N, 29.90; S, 19.70. $C_{11}H_{17}N_7S_2O$ requires: C, 40.40; H, 5.20; N, 30.00; S, 19.60%; mass spectrum: $m/z = 309$, yield = 81%.

Benzyl bis(thiosemicarbazone) (H_2L^4) was prepared using published procedures [21–23].

*2.4. Preparation of the palladium(II) complexes: [$PdCl_2(H_2L^2)$] (**1**), [$PdCl_2(H_2L^3)$] (**2**), [PdL^4]·DMF (**3**)*

A general procedure was followed: a suspension of the corresponding ligand (1 mmol) in MeOH was added with

stirring to a solution of lithium tetrachloropalladate(II) prepared in situ from palladium chloride(II) (1.2 mmol) and lithium chloride (4.4 mmol) in MeOH. The reaction mixture was stirred for 15 h at room temperature, the precipitate was filtered off, washed with MeOH and Et_2O, and dried in vacuo. [$PdCl_2(H_2L^2)$] (**1**): *Anal.* Found: C, 20.95; H, 3.00; N, 26.05; S, 13.40. $C_8H_{13}Cl_2N_9PdS_2$ requires: C, 20.15; H, 2.70; N, 26.45; S, 13.40%; orange solid; yield = 93%. [$PdCl_2(H_2L^3)$] (**2**): *Anal.* Found: C, 25.90; H, 3.50; N, 19.10; S, 12.50. $C_{11}H_{18}Cl_2N_7PdS_2O_{1.5}$ requires: C, 26.20; H, 3.40; N, 19.40; S, 12.70%; orange solid; yield = 63%. [PdL^4]·DMF (**3**): good quality green crystals suitable for X-ray analysis were obtained by recrystallization in DMF. *Anal.* Found: C, 45.20; H, 4.10; N, 19.00; S, 12.60. $C_{19}H_{21}N_7OS_2Pd$ requires: C, 45.29; H, 4.17; N, 19.47; S, 12.71%; yield = 71%.

2.5. Crystallography

A summary of the data collection and details of the structure refinement are given in Table 1. Single crystal data collection was performed at 293 K with a Siemens R 3m/V diffractometer by using a green prismatic crystal. The unit cell parameters were calculated by least-squares refinement of 25 reflections in the range $15 < 2\theta < 45°$. The data were corrected for Lorentz-polarization effects and for dispersion, and an empirical absorption correction was done [24]. The structure was solved by direct methods and subsequent Fourier syntheses with the SHELXTL V5 program [25]. In the final refinements all non-hydrogen atoms were refined anisotropically except for the C atoms which were refined isotropically. H atoms were included in calculated positions and treated as riding atoms using the SHELXTL V5 default parameters.

2.6. Drug cytotoxicity

Cell proliferation was evaluated by using a system based on the tetrazolium compound MTT which is reduced by living cells to yield a soluble formazan product that can be assayed colorimetrically [26]. Cells were plated in 96-well sterile plates, at a density of 10^4 cells/well in 100 μl of medium, and were incubated for 3–4 h. Compounds were added to final concentrations from 0 to 200 μM, in a volume of 100 μl/well. After 24 and 96 h, 50 μl of a freshly diluted MTT solution (1/5 in culture medium) was added to a concentration of 1 mg/ml into each well and the plate was incubated for 5 h at 37°C in a humidified 5% CO_2 atmosphere. Cell survival was then evaluated by measuring the absorbance at 520 nm, using a Whittaker 2001 microplate reader. IC_{50} values were calculated from curves constructed by plotting cell survival (%) versus compound concentration (μM). All experiments were made in quadruplicate.

Table 1
Experimental data for the crystallographic analysis of complex **3**

Formula	$C_{38}H_{42}N_{14}O_2Pd_2S_4$
Molecular weight	1067.90
Crystal system	triclinic
Space group	*P*1
a (Å)	10.258(5)
b (Å)	10.595(5)
c (Å)	11.189(5)
α (°)	97.820(5)
β (°)	108.140(5)
γ (°)	105.283(5)
U (Å^3)	1082.7(4)
λ (Mo Kα) (Å)	0.71069
Z	1
D_c (g/cm^3)	1.638
F(000)	540
Crystal size (mm)	0.2×0.2×0.1
μ (mm^{-1})	1.076
2θ Range (°)	2.05–25.00
hkl Ranges	−1 to 12; −12 to 12; −13 to 12
Independent reflections	4481
Observed reflections	4481
Largest difference peak, hole (e/Å^3)	0.827, −0.447
Absorption correction	empirical
System used	Siemens SHELXTL V5
Solution	direct methods
Refinement method	full-matrix least-squares on F^2
Data/restraints/parameters	4433/3/379
Final *R* indices [$I > 2\sigma(I)$]	*R*1 = 0.0361, *wR*2 = 0.0854
R indices (all data)	*R*1 = 0.0511, *wR*2 = 0.1022
Goodness of fit on F^2	0.965

2.7. Formation of compound:DNA complexes

The formation of the compound:DNA complexes was done by incubation in 10 mM $NaClO_4$ at 37°C of CT DNA (calf thymus DNA, Sigma) with a given volume of stock solution of compound **3** or *cis*-DDP until a value of $r_b = 0.1$ is achieved (molar ratio of Pt or Pd bound to nucleotides). The unreacted compound molecules were separated from the mixture by precipitation of the DNA with 2.5 volumes of EtOH and 0.1 volumes of 3 M sodium acetate, pH 4.8. Platinum and palladium atoms bound to CT DNA were quantified by total reflection X-ray fluorescence (TXRF) [27,28].

3. Results and discussion

3.1. Ligands and their metal-binding sites

Polydentate diprotic Schiff-base ligands H_2L^2, H_2L^3 and H_2L^4 can be found as thione or thiol forms (Fig. 1). Infrared scanning of the free ligands exhibits the ν(C=S) thioamide IV vibration at about 850 cm^{-1} indicating that they exist in the thione form. All show bands in the range 3400–3100 cm^{-1}. Assigning the two highest absorptions to ν(asym) and ν(sym) NH stretching frequencies, additional bands can arise from NH···N intermolecular hydrogen bonding. The negative shift of the thioamide bands upon complexation in com-

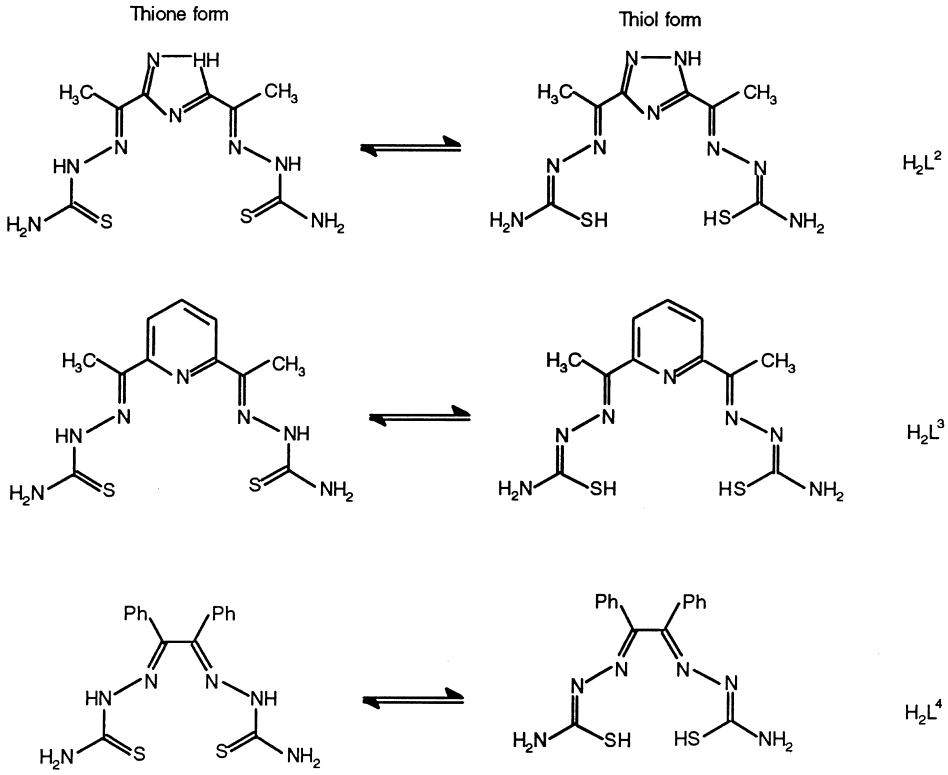

Fig. 1. Structural representations of H_2L^2, H_2L^3 and H_2L^4.

plexes **1** and **2** can be interpreted in terms of coordination through the sulfur atoms, in thione form, of the thioamide groups. Further evidence in support of the coordination of sulfur and chloride atoms is provided by the presence of new ν(Pd–S) and ν(Pd–Cl) bands (Table 2). Metal coordination of complex **3**, however, occurs through the sulfur, in thiol form via deprotonation of the –SH group, and iminic nitrogen atoms. This can be inferred from the red shift of the ν(C=N) vibration, the presence of a new band attributed to the ν(Pd–N) vibrations and the absence of any ν(SH) or ν(C=S) vibrations [29]. The well-resolved band at about 3117 cm^{-1} may be assigned to strong intermolecular hydrogen bonding. The SNNS coordination mode of the H_2L^4 ligand is confirmed by X-ray diffraction analysis.

3.2. ^1H NMR spectroscopy

Chemical shifts, in DMSO-d_6, for the free ligands and their palladium(II) complexes are given in Table 3. The changes in the spectrum of H_2L^2 under complexation are the following: (i) two singlets appear for methyl protons, thus indicating that the environments of these groups are slightly different, (ii) the protons of the $–NH_2$ groups are shielded and merge in a single signal, (iii) the protons assigned to –NH– thiosemicarbazone and triazole moieties are considerably shifted upfield.

The changes in the spectrum of H_2L^3 under complexation are the following: (i) two signals for two different NH groups appear, (ii) there are two signals for the $–NH_2$ groups shifted

Table 2
Selected vibrational bands (cm^{-1}) of ligands and palladium(II) complexes

	H_2L^2	**1**	H_2L^3	**2**	H_2L^4	**3**
ν(NH)	3386, 3326	3388, 3290,	3235	3385, 3245	3420, 3330,	3443, 3271,
	3171	3167	3158	3115	3250, 3150	3117
$\delta(NH_2)$	1630	1613	1619	1612	1610	1616
ν(CN)	1619	1613	1606	1594	1610	1624, 1616
Thioamide I	1503	1497	1505	1511	1465	1455
Thioamide IV	844	834	872	872, 702	840	–
ν(Pd–N)		–		–		480
ν(Pd–S)		440		416		430
ν(Pd–Cl)		368, 362		325		–

Table 3
^{1}H NMR and UV–Vis spectral data

	–CH_3	CH(Ph)	–$^4NH_2$	–^{2}NH–	–NH– (triazole)	λ_{max} (nm) (ε ($dm^3\ mol^{-1}\ cm^{-1}$))
H_2L^2	2.33(s)		8.59–8.31(m)	10.28(s)	14.54(s)	364 (350)
				10.77(s)		
1	2.2(s)		7.5(s)	8.6(s)	12.5(s)	321 (287)
	2.3(s)			9.4(s)		418 (583)
H_2L^3	2.38(s)		8.13(m)	10.29(s)		355 (580)
2	2.36(s)		9.37(s)	10.29(s)		321 (500)
	2.37(s)		9.20(s)	8.68(s)		426 (200)
H_2L^4		7.2–7.9(m)	8.4(s)	10.0(s)		391 (100)
				12.0(s)		
3		7.1(m)	7.8(s)	–		391 (24)
		7.2(m)				611 (900)

upfield, (iii) the signals due to the pyridine ring are quite different from those of the free ligand, which might be ascribed to the presence of isomers.

The spectrum of complex **3** shows the most pronounced changes with respect to the free ligand, the signals assigned to secondary amines disappear as a consequence of double deprotonation of the ligand in the complex. The protons of the aromatic and –NH_2 groups are shielded and shifted upfield. The $^4NH_2$ shift can be attributed to the increase of the N–H strength due to the coordination of the thiol sulfur to the palladium atom.

3.3. Electronic spectroscopy

Data are given in Table 3. Three d–d spin allowed singlet–singlet and three spin forbidden singlet–triplet transitions are predicted for square-planar complexes of palladium(II) but strong charge-transfer transitions may interfere and prevent the observation of some of the expected bands, which is actually observed in the electronic absorption spectra of the complexes. The prominent strong bands in the range 300–400 nm are assigned to a combination of intraligand and LMCT absorptions and d–d bands, which support the idea of a square-planar environment for the metal ions. Additionally, the spectrum of complex **3** exhibits a very intense band centered at 611 nm tentatively assigned to a spin-forbidden singlet–triplet transition which could have gained intensity through spin–orbit coupling [30].

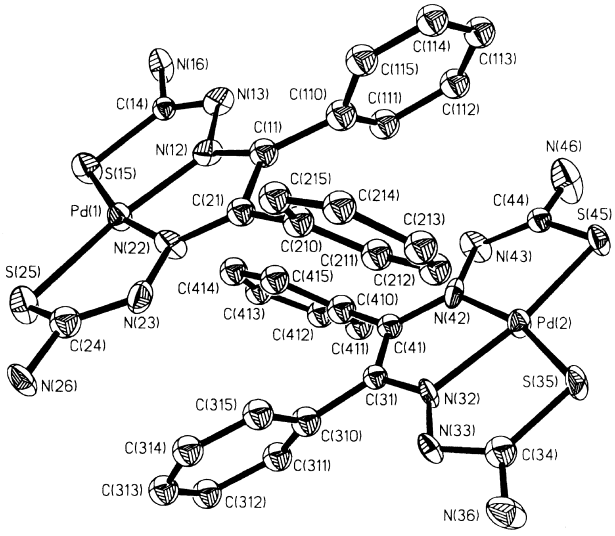

Fig. 2. Molecular structure of the PdL^4 complex.

3.4. Crystal and molecular structure

A drawing of complex **3** with the atomic numbering scheme is shown in Fig. 2 while selected bond lengths and angles are given in Table 4. The structure is characterized by the presence of two symmetry-independent molecules which do not differ significantly from each other, and two lattice dimethylformamide molecules. The palladium(II) atom has

Table 4
Selected bond lengths (Å) and angles (°)

Pd(1)–N(12)	1.91(2)	N(22)–N(23)	1.34(2)
Pd(1)–N(22)	1.96(2)	N(23)–C(24)	1.32(3)
Pd(1)–S(25)	2.290(6)	C(24)–N(26)	1.36(2)
Pd(1)–S(15)	2.299(7)	C(24)–S (25)	1.78(2)
Pd(2)–N(42)	1.99(2)	C(31)–N(32)	1.30(3)
Pd(2)–N(32)	2.03(2)	C(31)–C(41)	1.43(3)
Pd(2)–S(45)	2.256(5)	C(31)–C(310)	1.49(2)
Pd(2)–S(35)	2.277(6)	N(32)–N(33)	1.33(3)
C(11)–N(12)	1.35(3)	N(33)–C(34)	1.36(3)
C(11)–C(110)	1.48(3)	C(34)–N(36)	1.36(3)
C(11)–C(21)	1.55(3)	C(34)–S(35)	1.71(2)
N(12)–N(13)	1.42(2)	C(41)–N(42)	1.34(3)
N(13)–C(14)	1.32(3)	C(41)–C(410)	1.48(3)
C(14)–N(16)	1.31(3)	N(42)–N(43)	1.37(2)
C(14)–S(15)	1.80(2)	N(43)–C(44)	1.32(3)
C(21)–N(22)	1.29(3)	C(44)–N(46)	1.35(2)
C(21)–C(210)	1.46(3)	C(44)–S(45)	1.73(2)
N(12)–Pd(1)–N(22)	82.3(6)	N(42)–Pd(2)–N(32)	81.5(7)
N(12)–Pd(1)–S(25)	166.5(5)	N(42)–Pd(2)–S(45)	84.2(5)
N(12)–Pd(1)–S(25)	84.2(5)	N(32)–Pd(2)–S(45)	165.7(6)
N(12)–Pd(1)–S(15)	84.7(5)	N(42)–Pd(2)–S(35)	166.0(5)
N(12)–Pd(1)–S(15)	166.9(4)	N(32)–Pd(2)–S(35)	84.5(6)
S(25)–Pd(1)–S(15)	108.8(2)	S(45)–Pd(2)–S(35)	109.8(2)

a square-planar geometry surrounded by two sulfur and two nitrogen atoms, the L^4 ligand is in anionic form showing an *E,E* configuration about the C(14)–N(13) and C(24)–N(23) bonds. The organic molecule acts as tetradentate ligand. The coordination of the thiosemicarbazone results in the formation of three five-membered (PdSCNN, PdNCCN and PdNNCS) chelate rings, all of which are planar within experimental error [31].

A careful examination of the bond length data shows that the Pd–N_{iminic} and Pd–S distances (see Table 4) are comparable with those reported for other thiosemicarbazone palladium(II) complexes with strong Pd–N_{iminic} coordination [32–34] Å (e.g. Pd–N_{py} 2.053, Pd–N_{iminic} 1.971 and Pd–S 2.245 Å in bromo(2-acetylpyridine thiosemicarbazonato)palladium(II)) [35]. The loss of the protons originally bonded to ^{2}N produces a negative charge delocalized in the ligand system, which is consistent with the bond C–N distances, intermediate between formal single and double bonds [36], and C–S distances (see Table 4) which are in the range of single bond character being some of the largest found for thiosemicarbazone complexes (typical bond lengths being $C(sp_2)$–S 1.706 Å in $(MeS)_2C{=}C(SMe)_2$ and C=S 1.630 Å in naphthylphenylthioketone) [37,38]. This substantiates the displacement of the tautomeric equilibrium to the thiol form in the ligand.

An analysis of the packing diagram of $PdL^4 \cdot$DMF shows the existence of intermolecular hydrogen bonds, supporting the infrared stretching assignment given for NH. The hydrogen bonding network involves the uncoordinated nitrogen atoms of the ligand and the oxygen atoms of the two dimethylformamide molecules, the contact distances and angles being: $N(16)H\cdots N(33)^{I}$ (I: $x, y-1, z$) 3.023 Å, 160.6°; $N(36)H\cdots N(13)^{II}$ (II: $x, y+1, z$) 2.957 Å, 147.7°; and $N(26)H\cdots O(1)^{III}$ (III: $x, y, z+1$) 2.794, 153.0°; $N(46)H\cdots O(6)^{I}$ 2.916 Å, 165.4°.

As seen from Table 5, this complex shows geometric similarities to Cu(KTS) (Fig. 3) [39,40].

Table 5
Comparison of bond lengths (Å) and angles (°) of Cu(KTS) and PdL^4

	Cu(KTS)	[PdL^4]
C–N_{imine}	1.30, 1.29	1.35, 1.29
N–N	1.34, 1.35	1.42, 1.34
N–C(S)	1.33, 1.32	1.32, 1.32
C–S	1.76, 1.74	1.80, 1.78
C–N_{amine}	1.33, 1.36	1.31, 1.36
M–N	1.98, 1.96	1.91, 1.96
M–S	2.26, 2.27	2.29, 2.30
N–M–N	79.9	82.3
N–M–S	83.9, 84.3	84.2, 84.7
S–M–S	112.3	108.8

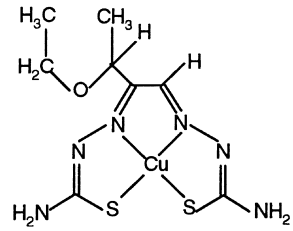

Fig. 3. Molecular structure of the Cu(KTS) complex.

3.5. Cytotoxic activity of compound *3*

Table 6 shows the cytotoxic activity of compound **3** and the antitumor drugs *cis*-DDP, adriamycin and etoposide against tumor cell lines sensitive to *cis*-DDP (HeLa, Vero), resistant to *cis*-DDP (Pam-*ras*), and normal cells (Pam 212) after treatment periods of 24 h (A) and 96 h (B). It may be observed in Table 6(A) that complex **3** has IC_{50} values between 20 and 78 μM depending on the cell line being more active than *cis*-DDP that exhibits IC_{50} values between 40 and 164 μM. Table 6(A) also shows that compound **3** is two times more active than *cis*-DDP in the *cis*-DDP-resistant cell line Pam-*ras* (IC_{50} values of 78 and 156 μM, respectively).

Table 6
IC_{50} mean values (μm) and standard deviations (SD) obtained for compound **3**, *cis*-DDP, adriamycin and etoposide against several tumor and normal cell lines at 24 h (A) and 96 h (B) drug-treatment periods

	IC_{50}(μM) ± SD			
Cell line	Vero	Pam 212	Pam-*ras*	HeLa
(A)				
3	47 ± 3	50 ± 2	78 ± 3	20 ± 2
cis-DDP	164 ± 4	120 ± 3	156 ± 6	40 ± 3
Etoposide	136 ± 10	76 ± 2	98 ± 4	54 ± 4
Adriamycin	156 ± 11	147 ± 6	165 ± 10	64 ± 6
Ligand (H_2L^4)	> 200	> 200	> 200	> 200
(B)				
3	16 ± 2	12 ± 1	20 ± 3	7 ± 1
cis-DDP	56 ± 4	40 ± 3	52 ± 4	13 ± 2
Etoposide	34 ± 4	27 ± 1	33 ± 2	18 ± 2
Adriamycin	52 ± 6	49 ± 4	41 ± 5	21 ± 3
Ligand (H_2L^4)	> 200	> 200	> 200	> 200

Moreover, compound **3** has a better in vitro therapeutic index (T.I.) than *cis*-DDP when comparing the IC_{50} in Pam-*ras* cells against Pam 212 cells (T.I. of 1.56 versus 1.30, respectively). Moreover, it is noteworthy that compound **3** exhibits higher cytotoxic activity than the clinically used drugs etoposide and adriamycin in all the tumor cell lines tested. Similar results were obtained for a drug-treatment period of 96 h although the IC_{50} values observed were on the average three to four times lower than those obtained at 24 h (Table 6(B)). On the other hand, the data of Table 6 indicate that the thiosemicarbazone ligand has poor cytotoxic activity. Altogether, these results suggest that in compound **3** the covalent binding of Pd(II) centers to bis(thiosemicarbazone) ligands results in a Pd-bis(thiosemicarbazone) clustered compound with new spectra of cytotoxic activity. Thus, from the cytotoxicity data presented in Table 6, it is concluded that compound **3** might have antitumor properties, particularly in view of the fact that it is quite active towards *cis*-DDP resistant tumor cells in which etoposide and adriamycin have poor or moderate cytotoxic activity.

*3.6. Analysis of the interaction of compound **3** with DNA secondary structure*

Because the cytotoxicity assays show that compound **3** is active in *cis*-DDP resistant Pam-*ras* cells it is likely that this novel Pd-thiosemicarbazone compound may have a biochemical mechanism of action different from that of *cis*-DDP. Thus, because it has been reported that DNA is the main cellular target of some platinum and palladium complexes with thiosemicarbazones [13,14], the interaction of compound **3** with the DNA secondary structure was analyzed.

Table 7
CD spectral data [a] for compound **3**:CT DNA and *cis*-DDP:CT DNA complexes formed at $r_b = 0.1$

Complex	θ_{max}	λ_{max}	θ_{min}	λ_{min}
Native CT DNA	410	278	−375	249
3:CT DNA	420	277	−374	248
cis-DDP:CT DNA	380	280	−374	249

[a] $[\theta] = \text{deg cm}^2\ \text{dmol}^{-1} \times 10^3$ (mean residual molecular elipticity).

*3.7. CD spectrum of compound **3**:DNA complexes*

The effect of binding of compound **3** on DNA secondary structure was determined by CD spectroscopy. The CD spectra and the wavelengths at which the maximum and minimum values of elipticity $[\theta]$ occur in control CT DNA, CT DNA incubated with compound **3** and in *cis*-DDP at $r_b = 0.1$ are shown in Fig. 4 and Table 7, respectively. It may be observed that the maximum value of elipticity of the positive band at 278 nm in native CT DNA increases from 410 θ to 420 θ units in compound **3**:CT DNA complexes. This change in elipticity is accompanied by a small change to shorter wavelength of the maximum of the positive band which is located at 277 nm in compound **3**:DNA complexes. In *cis*-DDP:CT DNA complexes the maximum value of elipticity of the pos-

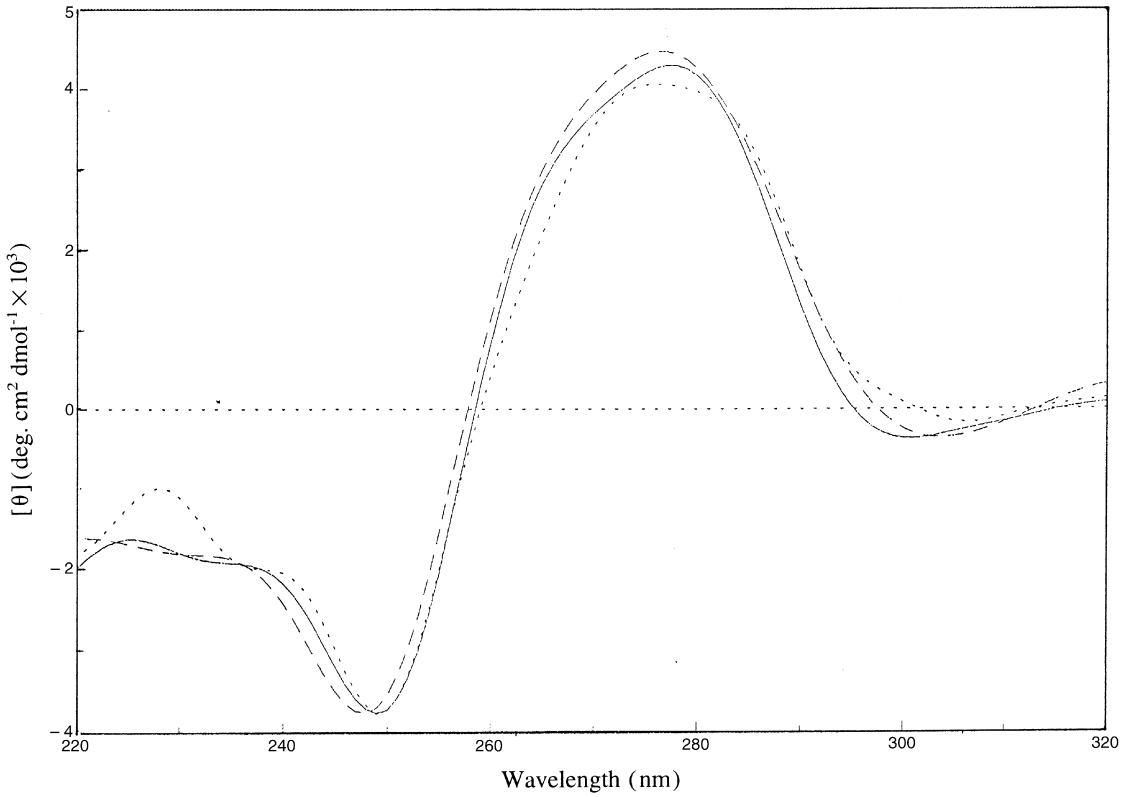

Fig. 4. CD spectra of control CT DNA (———) and of CT DNA incubated with compound **3** (— — —) and with *cis*-DDP (- - -) at $r_b = 0.1$.

itive band is located at 280 nm but decreases to 380 θ units. A new band with a maximum located at 228 nm appears in the CD spectrum of *cis*-DDP:CT DNA complexes indicating that the conservative nature of the CD curve is lost [41]. On the other hand, the minimum value of elipticity of the negative band present in native CT DNA at 249 nm decreases from -375 θ units to -374 θ units in compound **3**:CT DNA complexes. Moreover, a small displacement to shorter wavelength (248 nm) of the minimum value of elipticity of the negative band is induced by compound **3** in CT DNA. *cis*-DDP induces a similar decrease in the minimum of elipticity (-374 θ) of the negative band but without affecting the position of the minimum value (249 nm). These changes produced in the CD spectrum of CT DNA by compound **3** are indicative of an opening and rotation of the stacked bases on the DNA double helix but without affecting the conservative nature of the CD curve [42]. In addition, there is a slight displacement of the left half of the CD curve towards shorter wavelengths. The differences observed in the positive band of the CD spectra of compound **3**:CT DNA complexes relative to *cis*-DDP:CT DNA complexes and the new band located at 228 nm that appears in the CD curve of CT DNA modified by *cis*-DDP indicate that compound **3** produces on DNA secondary structure conformational changes that are different from those induced by *cis*-DDP.

Taking into account that compound **3** is active in *cis*-DDP resistant Pam-*ras* cells and, moreover, that it induces conformational changes on DNA secondary structure different from those induced by *cis*-DDP, it is most likely that part of the biochemical mechanism of action of this novel Pd-bis(thiosemicarbazone) complex may be due to its different mode of interaction with DNA relative to *cis*-DDP. In fact, because it is known that the reactivity towards DNA of platinum and palladium varies substantially it has been suggested that palladium compounds might circumvent cisplatin resistance in some tumor cell lines [3].

4. Supplementary material

Tables of crystallographic experimental details, atomic parameters, bond lengths, bond angles, anisotropic thermal parameters and hydrogen atom parameters are available from the authors.

Acknowledgements

We thank the Comisión Interministerial de Ciencia y Tecnología (Spain) for financial support (Projects MAT 95-0934-E and SAF-96-0041) and Dr Ramón y Cajal from Clínica 'Puerta de Hierro' of Madrid for his kind gift of Pam 212 and Pam-*ras* cells.

References

[1] S.B. Padhye, G.B. Kauffman, Coord. Chem. Rev. 63 (1985) 127.
[2] L.R. Kelland, Crit. Rev. Oncol. Hematol. 15 (1993) 191.
[3] N. Farrell, Transition Metal Chemistry Complexes as Drugs and Chemotherapeutic Agents. Kluwer, Dordrecht, 1989.
[4] A.S. Dobek, D. Klayman, E.T. Dickson, J.P. Scovill, C.N. Oster, Arzneim. Forsch. 33 (1983) 1583.
[5] S.B. Padhye, G.B. Kauffman, Coord. Chem. Rev. 63 (1985) 127.
[6] J. Shipman, S.H. Smith, J.C. Drach, D.L. Klayman, Antiviral Res. 6 (1986) 197.
[7] S.N. Pandeya, J.R. Dimmock, Pharmazie 48 (1993) 659.
[8] A.G. Quiroga, J.M. Pérez, I. López-Solera, J.R. Masaguer, A. Luque, P. Román, A. Edwards, C. Alonso, C. Navarro-Ranninger, Can. J. Med. Chem. 41 (1998) 1399.
[9] G. Wilkinson (Ed.), Comprehensive Coordination Chemistry, Pergamon, Oxford, 1987, and Refs. therein.
[10] A. Kraker, S. Krezoski, J. Schneider, D. Minkel, D.H. Petering, J. Biol. Chem. 260 (1985) 13710.
[11] W.E. Antholine, B. Kalyanaraman, D.H. Petering, Environ. Health Perspect. 64 (1985) 19.
[12] D.X. West, A.E. Liberta, S.B. Padhye, R.C. Chikate, P.B. Sonawane, A.S. Kumbhar, R.G. Yerande, Coord. Chem. Rev. 123 (1993) 49.
[13] A.G. Quiroga, J.M. Pérez, E.I. Montero, J.R. Masaguer, C. Alonso, C. Navarro-Ranninger, J. Inorg. Biochem. 70 (1998) 117.
[14] A.G. Quiroga, J.M. Pérez, I. López-Solera, E.I. Montero, J.R. Masaguer, C. Alonso, C. Navarro-Ranninger, J. Inorg. Biochem. 69 (1998) 275.
[15] Ch. Duan, B. Wu, T.C.W. Mak, J. Chem. Soc., Dalton Trans. (1996) 3485.
[16] P. Souza, A.I. Matesanz, V. Fernández, J. Chem. Soc., Dalton Trans. (1996) 3011.
[17] P. Souza, A.I. Matesanz, A. Arquero, V. Fernández, Z. Naturforsch., Teil B 94 (1994) 665.
[18] P. Souza, M.A. Mendiola, A. Arquero, V. Fernández, E. Gutierrez-Puebla, C. Ruiz Valero, Z. Naturforsch., Teil B 49 (1994) 263.
[19] R. Sánchez-Prieto, J.A. Vargas, A. Carnero, E. Marchetti, J. Romero, A. Durantez, J.C. Lacal, S. Ramón y Cajal, Int. J. Cancer 60 (1995) 235.
[20] J.M. Alonso, M.R. Marhn, J. Mendoza, T. Torres, J. Elguero, Heterocycles 26 (1987) 989.
[21] G.R. Gummerus, Soc. Sci. Fenn. Comment. Phys. Math. 32 (1966) 43.
[22] G.R. Gummerus, Chem. Abstr. 67 (1967) 63894y.
[23] M.K. Pandey, O.P. Pandey, S.K. Sengupta, S.C. Triphati, Polyhedron 6 (1987) 1611.
[24] N. Walter, D. Stuart, Acta Crystallogr., Sect. A 39 (1983) 158.
[25] SHELXTL PC version 5.0, Siemens Analytical X-ray Instruments, Madison, WI, 1995.
[26] M.C. Alley, D.A. Scudiero, A. Monks, M.L. Huresey, M.J. Czerwinski, D.L. Fine, B.J. Abbott, J.G. Mayo, R.H. Shoemaker, M.R. Boyd, Cancer Res. 48 (1988) 589.
[27] P. Wobrauscheck, Biol. Trace Elem. Res. 43–45 (1994) 65–71.
[28] V.M. González, P. Amo-Ochoa, J.M. Pérez, M.A. Fuertes, J.R. Masaguer, C. Navarro-Ranninger, C. Alonso, J. Inorg. Biochem. 63 (1996) 57.
[29] K. Nakamoto, Infrared and Raman Spectra of Inorganic and Coordination Compounds, 4th ed., Wiley-Interscience, New York, 1986.
[30] A.B.P. Lever, Inorganic Electronic Spectroscopy, 2nd ed., Elsevier, Amsterdam, 1984.
[31] E.W. Ainscough, A.M. Brodie, Coord. Chem. Rev. 27 (1978) 59.
[32] A. Bacchi, M. Carcelli, M. Cosla, P. Pelagatti, C. Pelizzi, G. Pelizzi, J. Chem. Soc., Dalton Trans. (1996) 4239.
[33] M. Bonamico, V. Fares, L. Petrilli, F. Tarli, G. Chiozzini, C. Riccucci, J. Chem. Soc., Dalton. Trans. (1994) 3349.
[34] K. Umakoshi, A. Ichimura, I. Kinoshita, S. Ooi, Inorg. Chem. 29 (1990) 4005.

[35] G.F. Sousa, C.A.L. Filgueiras, A. Abras, S.S. Al-Juaid, P.B. Hitchcock, J.F. Nixon, Inorg. Chim. Acta 218 (1994) 139.
[36] S. Zhu, F. Kou, H. Lin, C. Lin, M. Lin, Y. Chen, Inorg. Chem. 35 (1996) 5851.
[37] R.C. Collins, R.E. Davis, Acta Crystallogr., Sect. B 34 (1978) 283.
[38] P. Arjunan, V. Ramamurthy, K. Ventakesan, Acta Crystallogr., Sect. C 40 (1984) 556.
[39] M.R. Taylor, G.P. Glusker, E.R. Gabe, J.A. Minkin, A.L. Patterson, J. Am. Chem. Soc. 88 (1966) 1845.
[40] M.R. Taylor, G.P. Glusker, E.R. Gabe, J.A. Minkin, Bioinorg. Chem. 3 (1974) 189.
[41] R.W. Byrnes, M. Mohan, W.E. Antholine, R.X. Xu, D.H. Petering, Biochemistry 29 (1990) 7046.
[42] W.C. Johnson, M.S. Itzkowic, I. Tinoco, Biopolymers 11 (1972) 225.